



New lens on breast health: harnessing high-b-value synthetic diffusion-weighted imaging for breast lesion characterization

Serap Karabiyik¹
 Saime Ramadan²
 Emil Settarzade³
 Ali Ilker Filiz⁴
 Hatice Ozturkmen Akay⁵

¹Istanbul Training and Research Hospital, Clinic of Radiology, Istanbul, Türkiye

²Baskent University Istanbul Hospital, Department of Pathology, Istanbul, Türkiye

³Zollernalb Klinikum, Radiologie Abteilung, Balingen, Germany

⁴Baskent University Istanbul Hospital, Department of General Surgery, Istanbul, Türkiye

⁵Baskent University Istanbul Hospital, Department of Radiology, Istanbul, Türkiye

Corresponding author: Serap Karabiyik

E-mail: serapyucl@gmail.com

Received 21 December 2024; revision requested 27 January 2025; last revision received 26 March 2025; accepted 08 April 2025



Epub: 20.05.2025

Publication date: xx.xx.2025

DOI: 10.4274/dir.2025.253190

PURPOSE

This study aims to evaluate the diagnostic efficacy of synthetic diffusion-weighted imaging (sDWI) at various high b-values in distinguishing malignant from benign breast lesions and to compare its performance with that of conventional DWI (cDWI).

METHODS

After the exclusion of 22 lesions, 63 women (age range, 24–99 years; mean age, 53.7 ± 15.1 years) with 68 suspicious breast lesions on ultrasound who underwent multiparametric breast magnetic resonance imaging before biopsy between January 2021 and April 2023 were included in this retrospective study. According to the pathological results, lesions were classified as malignant or benign. Volumetric mask images were defined. The lesion signal/normal breast signal ratio [relative signal intensity (rSI)] was measured on different diffusion-weighted images (cDWI at b = 800 and 1500 s/mm²; sDWI at b = 1500–5000 s/mm²), and lesion SI on apparent diffusion coefficient (ADC) 0–800 and ADC0–1500 maps (mADC) was calculated. The diagnostic performances of these parameters were evaluated using a receiver operating characteristic curve analysis and the DeLong test in both the mass and non-mass lesion groups.

RESULTS

A total of 32 (47.06%) benign and 36 (52.94%) malignant lesions were identified. Malignant lesions exhibited significantly higher rSI values on cDWI800, cDWI1500, sDWI1500, sDWI2000, and sDWI3000 (P values: <0.001, <0.001, <0.001, <0.001, <0.001, 0.03) and lower mADC800 and mADC1500 values (P values: 0.01 and 0.03). In mass lesions, synthetic b1500 and conventional b1500 demonstrated diagnostic accuracy comparable with that of routine mADC800 and mADC1500. However, in non-mass lesions, high-b-value DWI maps (b ≥ 2000 s/mm²) significantly outperformed mADC and cDWI in differentiating malignant from benign lesions. The highest diagnostic accuracy in non-mass lesions was observed with rSIC4000 [area under the curve (AUC) = 0.87], whereas in mass lesions, rSIC1500 exhibited the highest diagnostic performance (AUC = 0.79).

CONCLUSION

The optimal b-value for DWI differs between mass and non-mass breast lesions, emphasizing the need for separate evaluation protocols. Although high-b-value sDWI provides limited added diagnostic value in mass lesions, it significantly improves malignancy detection in non-mass lesions, outperforming cDWI and ADC mapping.

CLINICAL SIGNIFICANCE

This study underscores the need for a tailored DWI protocol for optimal breast lesion characterization, particularly for non-mass lesions, where high-b-value synthetic imaging enhances diagnostic accuracy.

KEYWORDS

Breast, synthetic diffusion-weighted imaging, high-b-value, breast cancer, magnetic resonance imaging

Magnetic resonance imaging (MRI) is an imaging modality with high sensitivity, frequently used in breast imaging.¹ Diffusion-weighted imaging (DWI) is routinely added to protocols worldwide.² The addition of DWI to dynamic contrast-enhanced MRI (DCE-MRI) has been shown to improve the differentiation between malignant and benign breast lesions, thereby increasing specificity.^{3,4} However, the optimal b-values for DWI and the appropriate number of b-values to acquire remain subjects of debate.⁵⁻⁷ At low b-values, benign lesion signals cannot be sufficiently suppressed, whereas at high b-values, the signal-to-noise ratio (SNR) decreases. Taking both images simultaneously increases the acquisition time.⁸⁻¹⁰ The European Society of Breast Imaging recommends acquiring at least two b-values for breast DWI: a low b-value (0–50 s/mm²) and a high b-value (800 s/mm²). The selection of 800 s/mm² as the high b-value represents a balanced compromise, ensuring standardized imaging quality while maintaining sufficient SNR and diagnostic accuracy.⁶ Meanwhile, the Quantitative Imaging Biomarkers Alliance (QIBA) suggests acquiring a minimum of two b-values: a low b-value (0–50 s/mm²), an intermediate b-value (~100 s/mm²), and a high b-value (600–800 s/mm²). The QIBA emphasizes the inclusion of an intermediate b-value to enhance the precision of ADC measurements.¹¹

Synthetic DWI (sDWI) is derived from conventional DWI (cDWI) directly acquired using at least two distinct b-values. It has the potential to address the limitations of cDWI by effectively suppressing background signal at very high b-values, all without the need for additional scanning time.^{10,12} There are numerous studies on sDWI conducted on other organs, such as the liver and prostate.

Main points

- The optimal b-value for diffusion-weighted imaging (DWI) differs between mass and non-mass breast lesions.
- High-b-value synthetic DWI ($b \geq 2000$ s/mm²) demonstrated superior diagnostic performance in non-mass breast lesions compared with conventional apparent diffusion coefficient (ADC) maps and DWI ($b = 800$ s/mm²), whereas in mass lesions, it offered no diagnostic advantage over conventional DWI and ADC mapping.
- There is a need for tailored DWI protocols for mass and non-mass lesions to optimize breast cancer detection and lesion characterization.

However, a limited number of studies have investigated the diagnostic performance of sDWI.^{9,12-15}

The diagnostic utility of DWI in non-mass lesions is more variable, as non-mass enhancement often exhibits overlapping ADC values between benign and malignant cases, reducing specificity.^{16,17} Consequently, optimizing DWI protocols, including the selection of appropriate b-values and synthetic imaging techniques, is essential for improving lesion differentiation, with a particular focus on the mass or non-mass features of the lesions.

Therefore, the present study aims to investigate the diagnostic efficacy of sDWI with different high b-values for differentiating malignant breast lesions from benign ones and compare it with cDWI.

Methods

Study population and magnetic resonance imaging protocol

This single-center retrospective study was approved by the institutional review board (project no.: KA23/73) on March 2, 2023, and was conducted in compliance with the Health Insurance Portability and Account-

ability Act. Informed consent was waived due to the retrospective nature of the study.

Eighty-five women with 90 suspicious mass and non-mass breast lesions (Breast Imaging Reporting and Data System 4A–5) who underwent tru-cut biopsies between January 2021 and April 2023 were retrospectively evaluated. The patients underwent breast MRI either 1 month before or after the biopsy procedure. Indications for breast MRI included preoperative staging, high-risk patient screening, or equivocal mammogram and ultrasound results. After excluding 22 lesions, 68 consecutive suspicious lesions in 63 patients (age range: 24–99 years; mean age: 53.7 ± 15.1 years) were included in the study (Figure 1). The lesions were classified as malignant or benign based on pathological results from tru-cut or excisional biopsy.

All MRIs were performed in the prone position using a 4-channel breast coil on a 1.5T MRI scanner (MAGNETOM Avanto, Siemens Healthcare, Erlangen, Germany). As part of the routine clinical protocol, the following sequences were acquired: axial turbo spin-echo T1, turbo inversion recovery magnitude, and DCE-MRI (3D fat-saturated gradient-echo axial sequence) after intravenous injection of 0.2 mL/kg gadoterate meglumine (Dotarem).

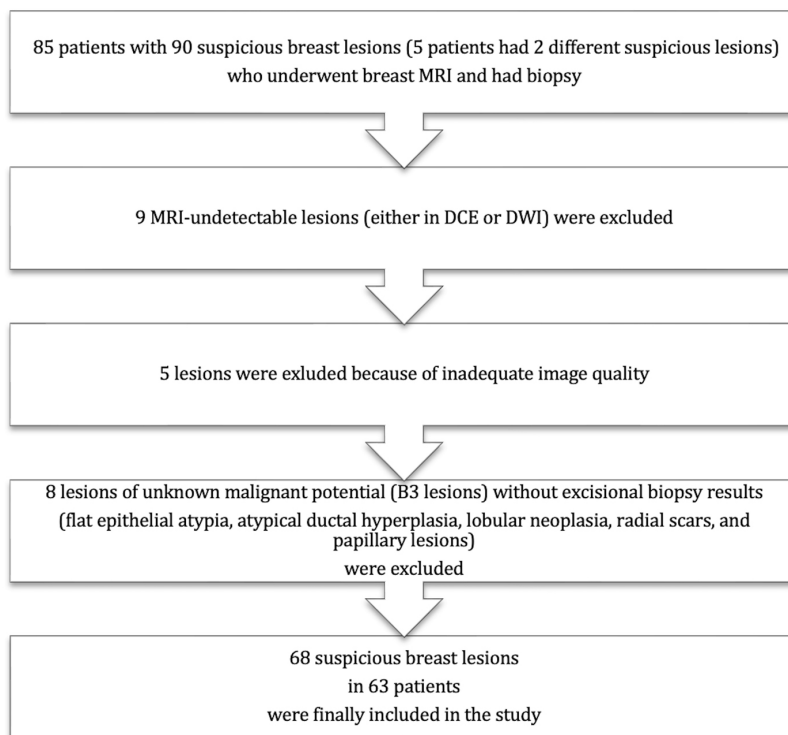


Figure 1. Flowchart of the patient inclusion and exclusion criteria. MRI, magnetic resonance imaging; DCE, dynamic contrast-enhanced; DWI, diffusion-weighted imaging.

Conventional and synthetic diffusion-weighted imaging and image analysis

DWI was acquired using spin-echo echo-planar imaging with spectral attenuated inversion recovery fat suppression and b-values of 0, 100, 800, and 1500 s/mm² (repetition time/echo time: 7,400/78 ms; slice thickness: 4 mm; number of excitations: 5; matrix size: 63 × 164; field of view: 340 × 390 mm; acquisition time: 6 minutes 32 seconds).

All DWI images were converted from DICOM format using the dcm2nii (Rorden, 2021). Noise was removed using the “dwide-noise” command in the MRtrix utility. Images with b-values of 0, 100, 800, and 1500 s/mm² were extracted using fsroi. Synthetic images with calculated b-values of 1500, 2000, 3000, 4000, and 5000 s/mm² were created using a monoexponential decay model via FSL 6.0.5 (FMRIB Software Library).¹⁸ Apparent diffusion coefficient maps (mADC) were also created with the same software.

A radiologist with 4 years of experience in breast radiology manually segmented the lesions on each slice of b = 0 DWI images, with the aid of DCE-MRI, avoiding necrotic, hemorrhagic, or cystic components using ITK-SNAP software (developed by the Penn Image Computing and Science Laboratory, University of Pennsylvania).¹⁹ For multifocal or multicentric tumors, only the index lesion was segmented. Volumetric mask images of the lesion and contralateral normal breast fibroglandular tissue were generated using the volume of interest (VOI) method based on b = 0 images and DCE with ITKs-SNAP (Figure 2). The VOI of the contralateral normal breast was carefully selected to minimize fatty tissue inclusion and match the volume of the mass lesion as closely as possible.

The average SI in the segmented lesion and contralateral normal breast was automatically calculated for each sDWI and cDWI image and mADC using “fslmaths.” relative signal intensity (rSI) for each DWI was calculated as follows:

$$rSI = \frac{(\text{mean SI of lesion})}{(\text{mean SI of contralateral normal breast})}$$

Both rSI values for different DWI maps and the mean SI for different mADC were analyzed.

Statistical analysis

The mean and standard deviation were calculated for each cDWI and sDWI in both

benign and malignant lesions, as well as in mass and non-mass subgroups. Based on the normality of the data, the Kolmogorov–Smirnov test was performed, followed by independent samples t-tests or Mann–Whitney U tests for between-group comparisons. Using receiver operating characteristic (ROC) curve analysis, the diagnostic efficacy of these values in malignant and benign lesions was evaluated. The DeLong test was used to assess whether sDWI images exhibited diagnostic superiority over cDWI and conventional mADC. Statistical analysis were performed using SPSS 22.0 and RStudio.

Results

The mean tumor size was 17.54 ± 5.23 mm (range: 6–80 mm). A total of 32 (47.06%) benign and 36 (52.94%) malignant lesions were identified. The characteristics of the tumors and patients are summarized in Table 1.

Malignant lesions exhibited significantly higher rSI values in cDWI800, cDWI1500, sDWI1500, sDWI2000, and sDWI3000 images and lower ADC800 and ADC1500 values (Table 2). Among the evaluated parameters, rSIC1500 demonstrated the highest diagnostic performance in ROC curve analysis [area under the curve (AUC) = 0.79], followed by rSIS1500 (AUC = 0.77). However, the DeLong test analysis revealed no statistically significant difference in AUC values between rSIC1500, rSIS1500, rSIS2000, ADC800, and ADC1500. Nevertheless, rSIC1500 was superior to rSIC800 and other high-b-value synthetic images (Table 2).

When mass lesions were analyzed separately, ADC800 and ADC1500 values were significantly lower in the malignant group, whereas rSIC800, rSIC1500, rSIS1500, and rSIS2000 were significantly higher (Figure 3). ROC curve analysis identified rSIC1500 as the most effective diagnostic parameter (AUC = 0.79), followed by rSIS1500 (AUC = 0.78). The DeLong test results indicated no significant differences in AUC values between cDWI1500, ADC800, ADC1500, rSIC800, rSIS1500, and rSIS2000. However, rSIC1500 was found to be superior to other high-b-value synthetic maps (Table 3).

For non-mass lesions, high-b-value images (b ≥ 2000 s/mm²) outperformed other parameters in distinguishing malignant from benign lesions. Among these, rSIC4000 exhibited the highest diagnostic accuracy (AUC = 0.87). The DeLong test analysis confirmed that rSIC4000 was significantly superior to mADC800 and mADC1500 and rSIC800 and rSIC1500 maps, although no significant differences were found between rSIC4000 and other synthetic maps (Table 3).

For mass lesions, the optimal cut-off value for rSIC1500 was 1.90 based on ROC curve analysis. At this threshold, rSIC1500 achieved a sensitivity of 61.3% and a specificity of 78.0%, with a positive predictive value (PPV) of 70.4% and a negative predictive value (NPV) of 55.6%.

For non-mass lesions, the optimal cut-off value for rSI4000 was 5.73. At this threshold, rSIS4000 demonstrated a sensitivity of 75% and a specificity of 83.3%, with PPV and NPV values of 75% and 83.3%, respectively.

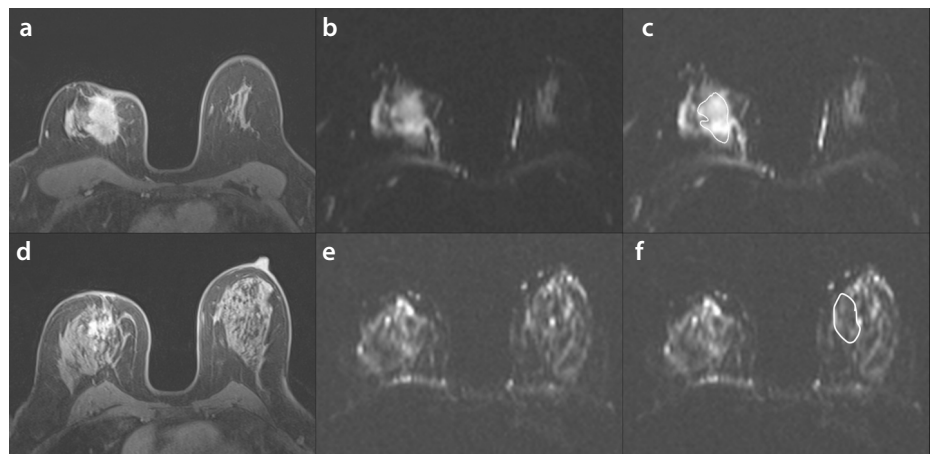


Figure 2. Segmentation process: An irregular mass in the upper quadrant of the right breast is visible in the contrast-enhanced axial image (a) and the b = 0 diffusion-weighted imaging (DWI) (b). The segmented area of the lesion in the b = 0 DWI sequence, used to create the mask image, is outlined with a white line (c). Additionally, the contrast-enhanced axial image (d) and the b = 0 DWI map (e) of the contralateral normal breast tissue, along with its segmentation marked by a white line, are shown (f).

	Malignant lesions: no. (%)	Benign lesions: no. (%)
Frequency	36 (52.94)	32 (47.06)
Mean diameter (mm) (min.-max.)	13.69 ± 6.46 (7–33)	27.64 ± 16.13 (6–80)
Shape		
Mass	31 (45.6)	26 (38.2)
Non-mass	5 (7.3)	6 (8.8)
Histopathological subtype	Invasive carcinoma of no special type 22 (32.3) Invasive lobular carcinoma 4 (5.9) 1 mixed IDC/ILC (1.5) Mucinous carcinoma 1 (1.5) Tubular carcinoma 1 (1.5) Mucoepidermoid carcinoma 1 (1.5) Ductal carcinoma <i>in situ</i> 5 (7.3) Focal microinvasive carcinoma on a background of papillary DCIS1 (1.5)	Fibroadenoma 12 (17.6) Fibrocystic changes 10 (14.7) Apocrine metaplasia 2 (2.9) Florid ductal hyperplasia 3 (4.4) Focal granulomatous mastitis 3 (4.4) Lobulocentric mastitis 1 (1.5) Papilloma 3 (4.4)
Grade		
1	3 (4.4)	-
2	15 (22.1)	-
3	12 (17.6)	-
Her-2 status		
Positive	5 (7.3)	-
Negative	31 (45.6)	-
Hormone receptor		
Positive	35 (51.5)	-
Negative	1 (1.5)	-
Number of lesions		
Multifocal	10 (14.7)	-
Multicentric	4 (5.9)	-
One mass	14 (20.6)	-

min.-max., minimum-maximum; no., number; IDC, invasive ductal carcinoma; ILC, invasive lobular carcinoma; DCIS, ductal carcinoma *in situ*.

	Benign (mean ± SD)	Malignant (mean ± SD)	<i>P</i>	AUC (95% CI)	<i>P</i> [†]
rSIC1500	1.4 ± 0.66	2.45 ± 1.24	<0.001*	0.79 (0.68–0.90)	-
rSIS1500	1.63 ± 1.04	2.93 ± 1.72	<0.001*	0.77 (0.66–0.88)	0.27
rSIS2000	1.76 ± 1.21	3.57 ± 2.87	<0.001*	0.73 (0.61–0.85)	0.08
rSIC800	1.64 ± 1.12	2.44 ± 1.19	<0.001*	0.72 (0.57–0.83)	0.03
ADC _{800x} 10 ⁻³	1.3 ± 0.42	1.06 ± 0.28	0.01 [†]	0.69 (0.56–0.82)	0.31
ADC _{1500x} 10 ⁻³	1.02 ± 0.37	0.85 ± 0.24	0.03 [†]	0.68 (0.55–0.82)	0.31
rSIS3000	2.64 ± 2.6	6.28 ± 8.63	0.03*	0.66 (0.53–0.79)	0.03
rSIS4000	6.16 ± 10.02	13.23 ± 25.15	0.10*	0.62 (0.48–0.75)	0.02
rSIS5000	21.89 ± 48.29	30.99 ± 71.97	0.30*	0.57 (0.43–0.71)	0.01

**P* values of the Mann–Whitney U test, [†]*P* values of the t-test, **P* values of the DeLong test comparing rSIC1500 with other parameters. AUC, area under the curve; CI, confidence interval; SD, standard deviation.

Discussion

The present study demonstrates that the optimal b-values for DWI differ between mass and non-mass breast lesions and that high-b-value synthetic images exhibit better diagnostic performance in non-mass breast lesions. In mass lesions, synthetic b1500 and conventional b1500 yielded comparable di-

agnostic performance to routine ADC800 and ADC1500 values. However, in non-mass lesions, high-b-value ($b \geq 2000$ s/mm²) DWI maps outperformed both mADC and cDWI images in diagnostic performance.

Previous research has suggested that higher b-values (1200–1800 s/mm²) enhance cancer detection and lesion conspicuity due

to the improved suppression of fibro-glandular tissue and benign lesion signals at higher diffusion weightings. Choi et al.⁹ reported that increasing b-values (800–1500 s/mm²) improved cancer detection rates and cancer-to-parenchyma contrast ratios (CPCR) for both sDWI and cDWI, with sDWI1500 demonstrating superior lesion conspicuity

Table 3. Comparison of the diagnostic values of synthetic and conventional diffusion-weighted imaging in mass and non-mass lesions

	Mass lesions					Non-mass lesions				
	Benig (mean ± SD)	Malignant (mean ± SD)	<i>P</i>	AUC (95% CI)	<i>P</i> ⁺	Benign (mean ± SD)	Malignant (mean ± SD)	<i>P</i>	AUC (95% CI)	<i>P</i> ⁺
rSIC800	1.92 ± 1.29	3.66 ± 3.01	0.08*	0.72 (0.58–0.86)	0.23	1.34 ± 1.01	3.49 ± 1.69	0.33*	0.70 (0.40–0.91)	0.03
rSIC1500	1.43 ± 0.73	2.47 ± 1.27	<0.001*	0.79 (0.66–0.88)	-	1.28 ± 0.47	2.65 ± 0.95	0.55	0.73 (0.43–0.92)	0.04
rSIS1500	1.70 ± 1.12	2.97 ± 1.76	0.001*	0.78 (0.65–0.88)	0.5	1.46 ± 0.96	3.02 ± 1.41	0.88	0.7 (0.36–0.93)	0.09
rSIS2000	1.92 ± 1.29	3.66 ± 3.01	0.008*	0.72 (0.59–0.83)	0.11	1.34 ± 1.01	3.49 ± 1.69	0.03	0.77 (0.43–0.96)	0.07
rSIS3000	3.17 ± 2.82	6.64 ± 9.21	0.17*	0.63 (0.49–0.75)	0.03	1.18 ± 1.11	4.80 ± 1.20	0.03	0.83 (0.43–0.96)	0.09
rSIS4000	7.98 ± 11.30	14.45 ± 26.91	0.35*	0.58 (0.44–0.71)	0.01	1.08 ± 1.15	6.79 ± 3.86	0.02	0.87 (0.54–0.99)	-
rSIS5000	29.66 ± 55.28	34.69 ± 77.03	0.97*	0.53 (0.39–0.66)	0.005	1.02 ± 1.12	9.85 ± 6.34	0.03	0.80 (0.46–0.97)	0.25
ADC _{800x} 10 ⁻³	1.27 ± 0.37	1.02 ± 0.27	0.007[†]	0.70 (0.57–0.82)	0.45	1.35 ± 0.36	1.07 ± 0.34	0.39	0.60 (0.28–0.87)	0.02
ADC _{1500x} 10 ⁻³	0.99 ± 0.33	0.81 ± 0.23	0.023[†]	0.70 (0.56–0.81)	0.43	1.07 ± 0.34	1.07 ± 0.09	0.67	0.63 (0.30–0.89)	0.02

**P* values of the Mann–Whitney U test, [†]*P* values of the t-test, ⁺*P* values of the DeLong test analysis. AUC, area under the curve; CI, confidence interval; SD, standard deviation; ADC, apparent diffusion coefficient.

and CPCR. Similarly, Bickel et al.¹⁴ found a significant increase in CPCR with b-values between 1000 and 2000 s/mm², identifying 1200–1800 s/mm² as optimal for image quality and lesion visibility. Park et al.¹³ reported that sDWI1500 enhances sensitivity without affecting predictive value, whereas Ahn et al.²⁰ observed that cDWI1000 provided better image quality compared with cDWI2000 and sDWI2000, despite superior lesion detection at cDWI2000. Naranjo et al.²¹ noted that synthetic b-values of 1200–1500 s/mm² offered the best lesion conspicuity, albeit with lower image quality. Additionally, Yilmaz et al.¹⁵ demonstrated that sDWI1500 outperformed cDWI800 in differentiating malignant from benign lesions, yielding higher sensitivity, specificity, and accuracy with fewer false positives. However, they did not compare higher b-values between sDWI and cDWI.¹⁵ None of these studies specifically analyzed mass and non-mass lesions separately. DWI may perform differently in distinguishing malignant lesions in mass versus non-mass lesions.^{16,17} Additionally, most studies in the literature have not used the DeLong test to compare differences in AUC values, limiting statistical insights into diagnostic performance.

Although there is still no universal consensus on the ideal b-value, our findings highlight the necessity of developing sepa-

rate DWI protocols for mass and non-mass lesions. Specifically, our results suggest that routine mADC and b800 DWI images provide diagnostic accuracy comparable with conventional b1500 and sDWI maps in mass lesions, questioning the added diagnostic value of high-b-value synthetic images in these cases. Conversely, our findings support the use of high-b-value DWI in non-mass lesions, as they demonstrated superior diagnostic performance in this subgroup. Incorporating sDWI images into routine breast MRI protocols may enhance diagnostic accuracy without extending acquisition times. Although not evaluated in the present study, prior research suggests that patient-related factors, such as breast density, may influence breast cancer detection rates on DWI.^{20,21} Moreover, sDWI offers radiologists greater flexibility by allowing lesion-specific and patient-specific selection of optimal b-values, thereby enhancing tailored imaging approaches.

Several limitations of this study should be acknowledged. First, its retrospective, single-center design and relatively small sample size limit the generalizability of the findings. Additionally, some patients underwent breast MRI after biopsy, which may have influenced the diffusion signal and affected imaging interpretation. The study population was also inherently biased, as it com-

prised patients undergoing breast biopsy for suspected breast cancer, potentially skewing the proportion of malignant lesions and impacting the study's sensitivity and specificity. Moreover, the predominance of hormone receptor-positive luminal-type tumors restricted the ability to perform subgroup analyses across different tumor subtypes. Lastly, the study focused solely on index lesions, which may not fully capture the complexities of multifocal or multicentric disease patterns.

In conclusion, the optimal b-values and the diagnostic performance of sDWI differ between mass and non-mass breast lesions. Although routine mADC and conventional b800 images offered diagnostic accuracy comparable with high-b-value synthetic images in mass lesions, high-b-value (b ≥ 2000) DWI maps significantly outperformed cDWI and ADC images in non-mass lesions. These findings suggest that a tailored DWI protocol is necessary for optimal lesion characterization, particularly for non-mass lesions where high-b-value imaging provides added diagnostic value. This study highlights the need for further research involving large patient populations and separate evaluations for mass and non-mass lesions to clarify the role of high-b-value sDWI in breast lesion assessment and to determine the optimal b-value for accurate diagnosis.

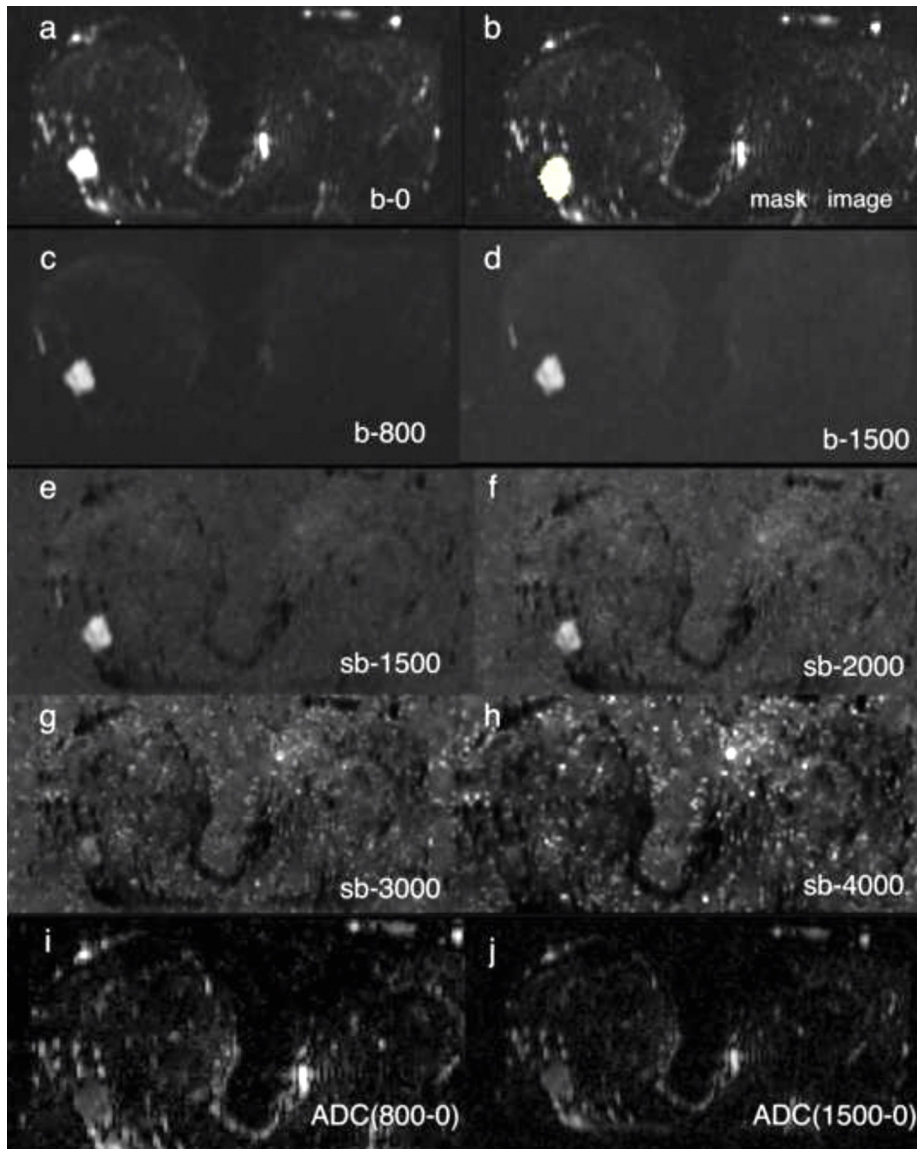


Figure 3. Conventional DWI (a, b, c, d) and synthetic DWI (e, f, g, h) images with different b-values and different ADC maps (i, j) of a patient with invasive NOS in the upper outer quadrant of the right breast are seen. The SNR, rSI, and lesion detectability decrease as the b-value gets very high (g, h). Low ADC signal was detected in ADC800 and ADC1500 images, as expected in malignant lesions. DWI, diffusion weighted imaging; ADC, apparent diffusion coefficient; SNR, signal-to-noise ratio; rSI, relative signal intensity.

Clinical significance

Implementing high-b-value sDWI into routine breast MRI protocols has the potential to enhance diagnostic accuracy, particularly for non-mass lesions without increasing scan time. By incorporating lesion-specific and patient-specific b-value optimization, radiologists can improve lesion characterization, potentially reducing unnecessary biopsies and improving clinical decision-making.

Footnotes

Conflict of interest disclosure

The authors declared no conflicts of interest.

References

1. Liberman L, Morris EA, Lee MJ, et al. Breast lesions detected on MR imaging: features and positive predictive value. *AJR Am J Roentgenol*. 2002;179(1):171-178. [\[Crossref\]](#)

2. Partridge SC, Nissan N, Rahbar H, Kitsch AE, Sigmund EE. Diffusion-weighted breast MRI: clinical applications and emerging techniques. *J Magn Reson Imaging*. 2017;45(2):337-355. [\[Crossref\]](#)
3. Pinker K, Moy L, Sutton EJ, et al. Diffusion-weighted imaging with apparent diffusion coefficient mapping for breast cancer detection as a stand-alone parameter: comparison with dynamic contrast-enhanced and multiparametric magnetic resonance imaging. *Invest Radiol*. 2018;53(10):587-595. [\[Crossref\]](#)
4. Spick C, Bickel H, Pinker K, et al. Diffusion-weighted MRI of breast lesions: a prospective clinical investigation of the quantitative imaging biomarker characteristics of reproducibility, repeatability, and diagnostic accuracy. *NMR Biomed*. 2016;29(10):1445-1453. [\[Crossref\]](#)
5. Ochi M, Kuroiwa T, Sunami S, et al. Diffusion-weighted imaging (b value = 1500 s/mm²) is useful to decrease false-positive breast cancer cases due to fibrocystic changes. *Breast Cancer*. 2013;20(2):137-144. [\[Crossref\]](#)
6. Baltzer P, Mann RM, Lima M, et al. Diffusion-weighted imaging of the breast—a consensus and mission statement from the EUSOBI International Breast Diffusion-Weighted Imaging working group. *Eur Radiol*. 2020;30(3):1436-1450. [\[Crossref\]](#)
7. Giannotti E, Waugh S, Priba L, Davis Z, Crowe E, Vinnicombe S. Assessment and quantification of sources of variability in breast apparent diffusion coefficient (ADC) measurements at diffusion weighted imaging. *Eur J Radiol*. 2015;84(9):1729-1736. [\[Crossref\]](#)
8. Woodhams R, Inoue Y, Ramadan S, Hata H, Ozaki M. Diffusion-weighted imaging of the breast: comparison of b-values 1000 s/mm² and 1500 s/mm². *Magn Reson Med Sci*. 2013;12(3):229-234. [\[Crossref\]](#)
9. Choi BH, Baek HJ, Ha JY, et al. Feasibility study of synthetic diffusion-weighted MRI in patients with breast cancer in comparison with conventional diffusion-weighted MRI. *Korean J Radiol*. 2020;21(9):1036-1044. [\[Crossref\]](#)
10. Blackledge MD, Leach MO, Collins DJ, Koh DM. Computed diffusion-weighted MR imaging may improve tumor detection. *Radiology*. 2011;261(2):573-581. [\[Crossref\]](#)
11. Shukla-Dave A, Obuchowski NA, Chenevert TL, et al. Quantitative imaging biomarkers alliance (QIBA) recommendations for improved precision of DWI and DCE-MRI derived biomarkers in multicenter oncology trials. *J Magn Reson Imaging*. 2019;49(7):e101-e121. [\[Crossref\]](#)

12. O'Flynn EA, Blackledge M, Collins D, et al. Evaluating the diagnostic sensitivity of computed diffusion-weighted MR imaging in the detection of breast cancer. *J Magn Reson Imaging*. 2016;44(1):130-137. [\[Crossref\]](#)
13. Park JH, Yun B, Jang M, et al. Comparison of the diagnostic performance of synthetic versus acquired high b-value (1500 S/Mm²) diffusion-weighted MRI in women with breast cancers. *J Magn Reson Imaging*. 2019;49(3):857-863. [\[Crossref\]](#)
14. Bickel H, Polanec SH, Wengert G, et al. Diffusion-weighted MRI of breast cancer: improved lesion visibility and image quality using synthetic b-values. *J Magn Reson Imaging*. 2019;50(6):1754-1761. [\[Crossref\]](#)
15. Yılmaz E, Güldoğan N, Ulus S, et al. Diagnostic value of synthetic diffusion-weighted imaging on breast magnetic resonance imaging assessment: comparison with conventional diffusion-weighted imaging. *Diagn Interv Radiol*. 2024;30(2):91-98. [\[Crossref\]](#)
16. Kul S, Eyuboglu I, Cansu A, Alhan E. Diagnostic efficacy of the diffusion weighted imaging in the characterization of different types of breast lesions. *J Magn Reson Imaging*. 2014;40(5):1158-1164. [\[Crossref\]](#)
17. Avendano D, Marino MA, Leithner D, et al. Limited role of DWI with apparent diffusion coefficient mapping in breast lesions presenting as non-mass enhancement on dynamic contrast-enhanced MRI. *Breast Cancer Res*. 2019;21(1):136. [\[Crossref\]](#)
18. Jenkinson M, Beckmann CF, Behrens TE, Woolrich MW, Smith SM. FSL. *Neuroimage*. 2012;62(2):782-790. [\[Crossref\]](#)
19. Yushkevich PA, Piven J, Hazlett HC, et al. User-guided 3d active contour segmentation of anatomical structures: significantly improved efficiency and reliability. *Neuroimage*. 2006;31(3):1116-1128. [\[Crossref\]](#)
20. Ahn HS, Kim SH, Kim JY, Park CS, Grimm R, Son Y. Image quality and diagnostic value of diffusion-weighted breast magnetic resonance imaging: comparison of acquired and computed images. *PLoS One*. 2021;16(2):e0247379. [\[Crossref\]](#)
21. Daimiel Naranjo I, Lo Gullo R, Saccarelli C, et al. Diagnostic value of diffusion-weighted imaging with synthetic b-values in breast tumors: comparison with dynamic contrast-enhanced and multiparametric MRI. *Eur Radiol*. 2021;31(1):356-367. [\[Crossref\]](#)